Journal of CO2 Utilization 86 (2024) 102891

Contents lists available at ScienceDirect

Journal of CO2 Utilization

journal homepage: www.elsevier.com/locate/jcou

Direct and green production of sterile aerogels using supercritical fluid technology for biomedical applications☆

María Carracedo-Pérez [a], Inés Ardao [b], Clara López-Iglesias [a], Beatriz Magariños [c], Carlos A. García-González [a,*]

[a] AerogelsLab, I+D Farma Group (GI-1645), Department of Pharmacology, Pharmacy and Pharmaceutical Technology, Faculty of Pharmacy, iMATUS and Health Research Institute of Santiago de Compostela (IDIS), Universidade de Santiago de Compostela, Santiago de Compostela E-15782, Spain
[b] BioFarma Research group, Department of Pharmacology, Pharmacy and Pharmaceutical Technology, Innopharma Drug Screening and Pharmacogenomics Platform, Centro Singular de Investigación en Medicina Molecular y Enfermedades Crónicas (CiMUS), Universidade de Santiago de Compostela, Santiago de Compostela E-15782, Spain
[c] Departamento de Microbiología y Parasitología, Aquatic One Health Research Center (iARCUS), Facultad de Biología-CIBUS, Universidade de Santiago de Compostela, Santiago de Compostela 15782, Spain

ARTICLE INFO

Keywords:
Supercritical CO_2
Sterilization
Biomaterials
Bioaerogels
Starch
Alginate

ABSTRACT

Aerogels based on natural polymers are of increasing interest in the biomedical field due to their biocompatibility, bioactivity, biodegradability and, in certain cases, extracellular matrix biomimicry. However, sterility has been a critical quality attribute limiting the use of aerogels in biomedicine. This work introduces a new and environmental-friendly technique based on the use of CO_2 called *in situ* sterilization that enables the manufacturing of sterile aerogel in a one-pot process. Starch aerogel cylinders and alginate aerogel beads enclosed within sterilization pouches were produced using this approach. The study involved the redesign of the flow diagram for aerogel production and the study of the effect of key parameters in the process (additive type and content, agitation, CO_2 flow regime type and duration) on the resulting material. The obtained materials were evaluated regarding their texture (helium pycnometry, N_2 adsorption-desorption analysis, SEM) and their sterility against three standardized bioindicators. Finally, the sterile aerogel materials were put in contact with NIH-3T3 cells assessing their cytocompatibility. Under the optimal operating conditions with 4.5 h of processing time, the aerogels were sterile, cytocompatible and had a porosity of *ca.* 80 % and a specific surface area of *ca.* 80 m^2/g and 200 m^2/g, for starch and alginate aerogels, respectively. Results allowed to identify the feasible operating region as well as the optimum processing values to obtain the typical nanostructure of aerogels, whilst ensuring suitable regulatory sterilization levels for aerogel implantation and cytocompatibility of the sterile material with fibroblastic cells.

1. Introduction

Aerogel synthesis is a top emerging technology in chemical engineering for the processing of advanced nanostructured materials for biomedical purposes [1,2]. These properties are of interest for drug delivery [3], wound healing [4], regenerative medicine [5,6] or oncotherapy [7]. The use of supercritical CO_2 ($scCO_2$) drying is the most common approach to remove the solvent without compromising the structural integrity of the gels. This process has been shown to enhance the porosity and specific surface area of different aerogel sources like starch or alginate [8,9]. Moreover, recent advances in aerogel formulation resulted in high versatility of external morphologies, porous structures and composition providing tailor-made biological performances for many administration routes (oral, nasal, pulmonary, skin) [3,10,11]. However, certain critical quality attributes needed for the biomedical use of aerogels are still underexplored or simply not reached yet. Among them, sterility or low microbial loads in aerogels are required by regulation in several cases, such as for implantable medical devices and combination products and for drug formulations intended for ocular and pulmonary delivery [12,13].

The production of sterile aerogels is not evident due to their complex nanostructure (high mesoporosity and tortuosity) and varied

☆ The work described in this manuscript is the subject of patent application number P202430533 led by Universidade de Santiago de Compostela

* Corresponding author.
E-mail address: carlos.garcia@usc.es (C.A. García-González).

https://doi.org/10.1016/j.jcou.2024.102891
Received 19 April 2024; Received in revised form 26 June 2024; Accepted 30 July 2024
Available online 9 August 2024

composition of this material that hinders the penetration capacity and, in many cases, excludes the use of high temperatures of certain conventional sterilization techniques [14–16]. The main alternatives to obtain sterile aerogels are (i) the aseptic processing of aerogels from sterile precursors, (ii) the post-sterilization of aerogels, and (iii) the aerogel preparation under sterilizing conditions (i.e. *in situ* sterilization). The first option, i.e. aseptic processing of aerogels, results in increasing manufacturing costs due to the higher costs of purchasing raw materials with certified sterility or of sterilization pretreatments, along with the higher processing costs of operating under aseptic conditions due to its increased complexity (including packaging). Then, the option of the downstream sterilization of aerogels results in an additional processing step leading to increased complexity and variability of results. Moreover, conventional sterilization techniques (ethylene oxide, gamma irradiation, thermal and UV) are either not able to reach the required sterility levels due to problems of penetrability in the intricate porous structures of aerogel, or cannot preserve the aerogel integrity in terms of physical properties (textural, mechanical) or of composition (changes in molecular weight, physicochemical degradation) with different grades of severity [17–19]. Alternatively, the supercritical post-sterilization of aerogels results in an effective treatment to kill microorganisms including spores under certain processing conditions, whilst preserving the physicochemical properties of the aerogels [16,20]. This technology not only provides an efficient solution for the sterilization of these complex polymeric materials, but it is also an innovative application for the reuse of CO_2, a by-product of various industrial sectors, as others currently in use for e.g. extraction of chemical compounds or processing of new materials for energy storage [21,22]. The sterilizing properties of $scCO_2$ arises from a myriad of mechanisms interfering the microbial metabolism (inactivation of decarboxylase enzymes, carbonates formation) and extracting/altering key components of the cell (increased permeability of membranes, extraction of membrane and cytoplasmic lipids), but being CO_2 diffusion into the cells and the acidification of the medium the main root causes [13,23]. Finally, the *in situ* sterilization of aerogels during their production at the required biomedical sterility levels for implantation (i.e. SAL-6) would be of high significance as it has not been reached so far and would open novel perspectives for the use of these materials in biomedicine. This *in situ* sterilization strategy is also regarded as an auspicious and feasible solution from technological and economic perspectives not achieved so far, especially considering that aerogels are usually obtained by a $scCO_2$-assisted process, i.e. the supercritical drying of gels.

The hypothesis of this work is that sterile aerogels at SAL-6 levels can be produced after the supercritical drying without further post-processing, provided that convenient changes in the drying process are carried out. Accordingly, the multiagent behaviour of $scCO_2$, i.e. extracting and sterilizing agent, is herein exploited as a technological platform for the integrated processing of sterile polysaccharide aerogels at SAL-6 levels, which represents the novelty of this work. On one hand, the low-temperature supercritical drying is the benchmark for aerogel production and consisting of the extraction of the liquid phase, usually ethanol, in the gel using a flow of $scCO_2$ under mild temperature and pressure conditions (typically, 37–50 ºC and 90–180 bar). These mild operating conditions allow the use of this technology in a variety of biomedical applications, including the processing of thermolabile polymers and temperature-sensitive drugs [24]. Several mass transfer mechanisms (spillage, convection and diffusion) are involved in this process with varying major contributions during the process [8,25–27]. The overestimation of the drying duration is a typical practice as this ensures an effective drying and it usually does not influence the end textural properties of the aerogel, except for certain cases like starch aerogels where this rule-of-thumb is detrimental for the aerogel network [25,28]. On the other hand, the sterilizing properties of $scCO_2$ are effective for most viruses and yeasts, as well as for Gram-positive and Gram-negative bacteria in their vegetative forms [17,29,30]. However, $scCO_2$ is not able to inactivate alone all bacterial species at their most resistant forms, i.e. as spores, at relevant biomedical sterility levels. $scCO_2$ should work in tandem with chemical additives (typically hydrogen peroxide and peracetic acid) at ppm levels to successfully kill *Bacillus pumilus*, the most resistant microorganism to the supercritical sterilization treatment [31].

In this work, the *in situ* production of sterile aerogels was carried out for the first time by means of the integration of the supercritical drying and supercritical sterilization processes assisted by the use of CO_2. Ready-to-use alginate aerogel beads and starch aerogel cylinders enclosed within sterilization pouches were obtained for biomedical purposes. The engineering study included the redesign of the process flow diagram for aerogel production and the tuning of the processing parameters (additive type and content, agitation, CO_2 flow regime type) to incorporate the sterilization process within the supercritical drying process. The efficacy of the process was evaluated from the material performance and the sterilization perspectives. The obtained aerogels were characterized regarding their textural properties by N_2 adsorption-desorption tests, helium pycnometry and scanning electron microscopy (SEM), and compared to aerogels processed without sterilization. The sterilization was microbiologically evaluated using endospore strips of *Bacillus stearothermophilus, Bacillus atrophaeus* and *B. pumilus*, which is the bioindicator (BI) of the supercritical process, subjected to these supercritical conditions [32]. Furthermore, to ensure that sterile material was not contaminated with toxic residues from the process, such as residual traces of H_2O_2, both types of aerogels were subjected to cytotoxicity tests, in which cells viability was measured after 24 and 48 h.

2. Materials and methods

2.1. Materials

Alginic acid sodium salt from brown algae (guluronic/mannuronic acid ratio of 70/30, MW=403 kDa) was supplied by Sigma Life Science (Irvine, UK). Native maize starch (Starch Amylo N-400) with a 52.6 % of amylose content, labeled as raw, was provided by Roquette Frères S.A. (Lestrem, France). Calcium chloride anhydrous ($CaCl_2$, >99 % purity) and absolute ethanol (EtOH, >99.9 % purity) were provided by Scharlab (Barcelona, Spain) and VWR (Radnor, PA, USA), respectively. CO_2 (99.8 % purity) was supplied by Nippon Gases (Madrid, Spain) and hydrogen peroxide (H_2O_2) 30 % (v/v) by Sigma-Aldrich (Madrid, Spain). Water was purified using reverse osmosis (resistivity > 18 MΩ·cm, Milli-Q, Millipore®, Madrid, Spain).

Sterility biological indicators: *B. pumilus* (ATCC 27142) spore strips (10^6 spores/strip) and *B. stearothermophilus* (ATCC 7953) spore strips (10^6 spores/strip) were purchased from Sigma-Aldrich (Madrid, Spain), whereas *B. atrophaeus* (cell line 9372) spore strips (2.4×10^6 spores/strip) were obtained from Crosstex International (Rush, NY, USA). Trypticase soy broth (TSB) and trypto-casein soy agar (TSA) medium were purchased from BIOKAR Diagnosis (Pantin, France). Ultrapure nitrogen (N_2 > 99 % purity) supplied by Nippon Gases (Madrid, Spain) was used for the adsorption-desorption textural analyses.

2.2. Preparation of alcogels

Alginate hydrogel beads were prepared by external ionic gelation using the dripping method [33,34]. Briefly, alginate powder was dissolved in distilled water with magnetic stirring (300 rpm) overnight to obtain a final concentration of 2.0 % (w/v). Then, 20 mL of the alginate solution was transferred to a syringe with 2 mm nozzle diameter for the formation of the alginate beads by dropping it into a 50 mL bath of 150 mM $CaCl_2$ solution from a height of 20 cm and at a constant flow rate of 1.4 mL/min using a syringe pump (AL-1000, World Precision Instruments, Sarasota, FL, USA). After 2 h of ageing in $CaCl_2$ solution, the gel particles were immersed in EtOH for solvent exchange.

Starch hydrogel monoliths were obtained by thermal gelation in moulds [16]. Briefly, aqueous starch 8 % (w/v) dispersions were

prepared and subjected to a thermal treatment at 121°C and 1.1 bar for 20 min for starch dissolution. After dosing the starch solutions in cylindrical moulds (6 cm of height and 12 mm of diameter), starch gelation took place. Starch gels were stored at 4°C for 48 h for retrogradation and then immersed in EtOH and cut in cylinders of 3.5 mm length.

In both alcogel cases, two consecutive solvent exchange steps were performed at a frequency of 24 h to replace water by EtOH in the gel structure.

2.3. Production of non-sterile aerogels by supercritical drying

Starch and alginate alcogels were subjected to a supercritical drying treatment to obtain the aerogels. Briefly, alcogels were placed into a 100-mL autoclave (TharSFC, Pittsburg, PA, USA; item 7 in Fig. 1) soaked in EtOH and then put in contact with $scCO_2$ [33]. The gel samples were previously enclosed in thermosealed pouches, as preliminary tests (not showed) confirmed that drying them in such pouches did not have an impact on the inner porous structure of the aerogels.

The supercritical drying process is carried out at 39 °C under three different and consecutive regime steps as sketched in Fig. 2A: (i) a dynamic regime at 120 bar with 7 g/min of CO_2 flow during 2 h; (ii) a static regime at 135 bar under $scCO_2$ without flow for 1 h; (iii) a second dynamic regime at 120 bar with $scCO_2$ flow at 5 g/min during 1.5 h. Finally, the autoclave was depressurized at a rate of 1 bar/min until reaching atmospheric pressure. Henceforth in the text, this protocol for the production of non-sterile aerogels will be referred to as "conventional drying".

2.4. In situ sterilization during aerogel production

For the *in situ* production of sterile aerogels, the sterilization treatment was integrated into the conventional aerogel drying procedure. The autoclave thermosealed pouches (Soplaril Hispania, Barcelona, Spain) were firstly filled with alginate and starch alcogels. Then, the *in situ* sterilization drying process involved a conventional $scCO_2$ drying with the same three steps as described in Section 2.3, but with slight modifications in the depressurization rate, in the procedure in step ii, and in the addition of the chemical additive for sterilization (Fig. 2B). On one side, the depressurization rate was increased to 3 bar/min in accordance to sterilization tests in the literature [31]. Meanwhile, in step ii, the pressure was increased 5 bar, and the durations tested in this step varied from 1 to 3 h depending on the trial. Moreover, the additive (H_2O_2) was added at the beginning of this step in different concentrations (1700–5000 ppm) to evaluate the inactivation of microorganisms' efficacy. The injection of the additive was performed at 7 g/min through a new line implemented in the system that is a tube of 2.2 mm of internal diameter (thick black lines in Fig. 1), which allowed the addition of the chemical additive at the bottom of the autoclave once it was already under pressure. The presence of the additive during the process is represented as a green line in Fig. 2B. For improving H_2O_2 homogenization, the stirring effect was evaluated at 700 rpm either during step ii only, or during both steps ii and iii.

2.5. Microbiological evaluation of the sterilization treatment efficacy

The efficacy of the *in situ* sterilization treatments was evaluated using standard BIs: *B. stearothermophilus* (standard BI of steam sterilization [35]), *B. atrophaeus* (standard BI of ethylene oxide sterilization [36]) and *B. pumilus* (standard BI of radiation sterilization [37]). In each *in situ* experiment, dry spore strips of all three BIs were placed in the autoclave together with the alcogels and subjected to the same sterilization tests (see Section 2.4). After processing, the spore strips were collected and seeded in TSB medium. Following this, *B. atrophaeus* and *B. pumilus* were incubated at 37 °C and *B. stearothermophilus* at 55 °C for 7 days. Bacterial growth was evaluated by optical turbidity measurement in the tubes and confirmed by seeding in TSA plates daily for 7 days. The treatment conditions were considered sterilizing when there was no bacterial growth after 7 days of incubation in none of the BIs, resulting in sterilization levels of SAL-6 for all BIs. TSB medium (microbiological negative control) and untreated spore strips (microbiological positive control) seeded in TSB were incubated at the same conditions as controls of the process.

2.6. Physicochemical characterization of sterilized aerogels

The bulk density of starch aerogel cylinders (ρ_{Bulk}) and the envelope density of the alginate aerogel beads (ρ_{Env}) were determined by measuring the dimensions and weight of the aerogels. The skeletal density of the aerogels (ρ_{Skel}) was determined using a helium-pycnometer (Quantachrome, Boynton Beach, FL, USA) at room

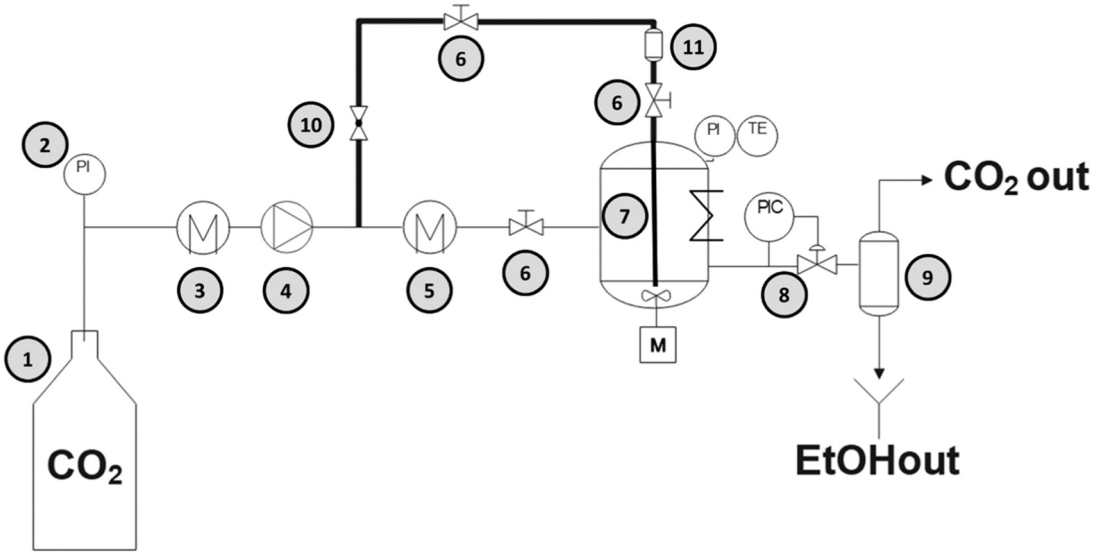

Fig. 1. Process flow diagram of the equipment used for the $scCO_2$ drying and sterilization treatments for gels. A new process line (thick black lines) was implemented to allow the *in situ* addition of the chemical sterilization additive (H_2O_2) in the pressurized autoclave. Legend: 1. CO_2 supply; 2. Pressure indicator; 3. Chiller; 4. Dual piston CO_2 pump; 5. Heat exchanger, 6. Needle valves; 7. Pressure vessel equipped with magnetic stirring and heating jacket; 8. Backpressure regulator; 9. Separator-collector vessel; 10. Ball valve; and 11: Additive vessel equipped with a plug where H_2O_2 is pre-loaded and then injected.

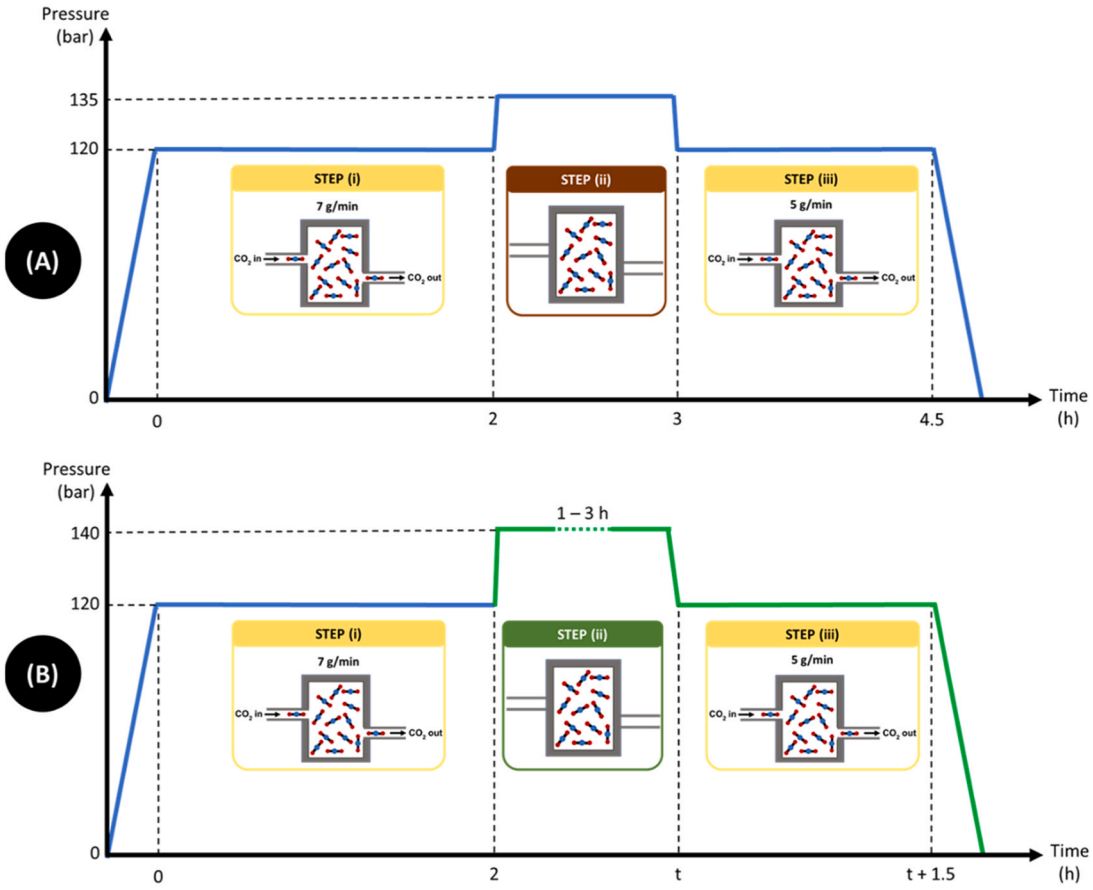

Fig. 2. Pressure-time process profiles of (A) a conventional drying for the production of aerogels and (B) an *in situ* sterilization upon drying process to obtain sterile aerogels. The green line represents the period with presence of H_2O_2 in the equipment.

temperature (25 °C) and 1.01 bar. Values were obtained from five replicates (standard deviation < 5 %). The resulting overall porosity (ε) was calculated according to Eq. (1):

$$\varepsilon(\%) = \left(1 - \frac{\rho_i}{\rho_{Skel}}\right) x \quad 100 \tag{1}$$

where ρ_i is *bulk* or *envelope* density for starch aerogel cylinders and alginate aerogel beads, respectively.

The textural properties of the aerogels were determined by N_2 adsorption-desorption analysis (ASAP 2000 Micromeritics Inc, Norcross, GA, USA). Prior to analysis, the samples were degassed under vacuum (<1 mPa) for 24 h with a degassing temperature of 40 °C and 60 °C for alginate and starch aerogels, respectively. The specific surface area (A_{BET}) of the aerogels was determined by the Brunauer-Emmett-Teller (BET) method, whereas the Barrett-Joyner-Halenda (BJH) method was used to determine the mean pore diameter (D_P) from the desorption branch of the isotherm. The same BJH-method was used to determine the specific mesopore volume ($V_{P,\ meso}$). The total void volume (V_v) was calculated from Eq. (2). Specific macropore volume ($V_{P,\ macro}$) was calculated by difference between V_v and $V_{P,\ meso}$.

$$V_v(cm^3/g) = \frac{1}{\rho_i} - \frac{1}{\rho_{Skel}} \tag{2}$$

Texture of aerogels was studied by scanning electron microscopy (SEM) using a FESEM UltraPlus microscope (Zeiss, Jena, Germany). Aerogels were previously sputter-coated with a 10 nm layer of iridium to improve the contrast (Q150 T S/E/ES equipment, Quorum Technologies, Lewes, UK).

Non-sterile and *in situ* sterilized alginate and starch aerogels were analyzed by attenuated total reflectance/Fourier-Transform Infrared Spectroscopy (ATR/FT-IR) in a Varian FT-IR 670 with a Gladi-ATR accessory (Varian, Palo Alto, CA, USA). The aerogels were characterized in the mid-IR spectrum range (400–4000 cm^{-1}) using 32 scans at a resolution of 4 cm^{-1}.

2.7. *In vitro compatibility studies*

The cytocompatibility of the bioaerogels was tested with the NIH-3T3 cell line (ATCC: CRL-1658) [38]. The cells were seeded in 24-well plates containing 500 μL DMEM supplemented with 10 % bovine serum and 1 % penicillin-streptomycin (12000 cell per cm^2 for 24 h and 8000 cell per cm^2 for 48 h) and incubated at 37°C in a humidified atmosphere supplemented with 5 % CO_2. After 24 h, the materials were placed in 24-well culture inserts (PET track-etched membrane with 0.4 μm pore size) in triplicate, 100 μL of medium was added on top and they were introduced in the well plate. To ensure that potential H_2O_2 residues will be dissolved in the medium, the viability was also measured after 48 h. Negative controls consisting of cells without material were incubated under the same conditions and in triplicate for all formulations. To assess the cytotoxicity of the blank samples (unsterile aerogels), these bioaerogels were firstly sterilized by UV for 30 min and then placed in the wells with cells using culture inserts.

Cell viability was assessed using the resazurin assay that measures the mitochondrial function of metabolic active cells. The material was removed from the cells after 24 and 48 h of incubation, the culture medium was aspirated and 300 μL of 44 μM resazurin were added in each well. After 3 h of incubation under identical conditions, fluorescence was measured at an excitation wavelength of 544 nm and an emission wavelength of 590 nm in a microplate reader (Infinite® M200, Tecan Group Ltd., Männedorf, Switzerland).

2.8. Statistical analysis

Results were expressed as mean ± standard deviation. Statistical analyses of textural properties and cell viability were obtained using 2-way ANOVA test, followed by the post-hoc Tukey HDS multiple comparison test using GraphPad Prism v.8.0.2 (GraphPad Software, Boston, MA, USA).

3. Results and discussion

3.1. Preliminary studies and space design definition for the integrated sterilization within the aerogel production

Previous experiments conducted in our laboratory have showed that conventional supercritical drying, which is carried out in the presence of ethanol in alcogels, was not enough to attain the inactivation of any of the three BIs tested (*Blank* sample in Table 1). In the literature, other attempts to sterilize with $scCO_2$ without additives can be found [12,16]. However, these attempts did not reach SAL-6 levels for the most resistant bioindicators used in this work or required more aggressive working conditions than the ones herein presented. Other studies have shown that the use of additives, such as H_2O_2, improves the effectiveness of sterilization [13,39].

This work aims to successfully integrate the sterilization process into the drying process while simplifying the design space for the experiments. Many variables are involved in the $scCO_2$ sterilization process, such as working pressure and temperature, stirring rate, exposure time and regime, concentration of chemical additives, and depressurization rate [13,17]. In a previous research to obtain ready-to-use PCL implants by $scCO_2$ sterilization [31], the sterilization conditions were set at 140 bar and 39 °C, in the presence of different amounts of H_2O_2 with exposure times ranging from 1 to 5 h and a depressurization rate of 13.3 bar/min. A 2.5-hour exposure was enough to inactivate the most resistant microorganisms and thus achieve sterilization of this type of porous material. In an attempt to simplify the space design of this work, these previously reported conditions (H_2O_2, 39°C, 140 bar, 2.5 h) reaching sterility for *B. pumilus* were set as initial guess to directly integrate sterilization into the supercritical drying process.

Some tests at low depressurization rates (1 bar/min) were not able to remove the additive during the sterilization process, whereas high rates (13.3 bar/min) collapsed the inner structure of the material (not showed). An intermediate depressurization rate of 3 bar/min was set as trade-off solution close to the values of the conventional supercritical drying process, without residual H_2O_2 in the aerogels and with good textural properties.

Since the presence of an additive is necessary for sterility, H_2O_2 was initially attempted to be incorporated before the pressurization of the autoclave. However, sterility was not achieved, presumably due to the premature elimination of H_2O_2 from the autoclave by the CO_2 flow already during the step i of the process (Fig. 2B). Consequently, the injection of H_2O_2 was established at the beginning of the step ii. For that purpose, a new line was implemented in the experimental setup to allow the injection of the additive once the autoclave was pressurized (thick lines in Fig. 1). This injection procedure allowed to mimic the operational time conditions needed for supercritical sterilization either with a prolonged step ii (Fig. 2B) or, preferably, in a combined sterilization during the steps ii and iii of the stand-alone supercritical drying process. In the latter case, it is hypothesized that H_2O_2 will dissolve in the $scCO_2$ during the step ii thus initiating the inactivation process, based on the solubility data of H_2O_2 in $scCO_2$ in the literature [40]. Then, the CO_2 flow would extract lipids from the cell membranes during the step iii to increase the sterilization efficiency and would also remove H_2O_2 residues from the material.

This *in situ* process to obtain sterile aerogels by integrating supercritical sterilization within the supercritical drying process does not entail significant modifications in the conventional drying treatment. The presence of agitation and the injection of a chemical additive during the process are the major processing changes. The selected protocol may somehow largely guarantee the structural, textural and physicochemical properties of the material as will be assessed in the following experimental sections. Based on this space design and following these procedure guidelines, the complete inactivation of the three BIs tested was achieved during the supercritical drying process under different conditions.

In the following sections, the effects of additive concentration, exposure time and stirring on the sterilization efficacy (Section 3.2), material properties (Section 3.3) and material cytotoxicity (Section 3.4) were evaluated.

The sterilization tests were denoted as *X_Y_C*. *X* is the stirring applied in the experiment: no stirring samples are named as N, stirring just in the step ii are named as B and stirring in steps ii and iii are named as BS. The second character, *Y*, is the step ii duration in hours, and the last character, C, is the amount (in ppm) of H_2O_2 added in the test. The notation of trials tested with 3300 ppm of H_2O_2 were shortened as *X_Y*.

3.2. Microbiological evaluation of the sterilization efficacy of the integrated process

3.2.1. Additive concentration effect

The additive concentration needed for an effective sterilization was initially studied in the 1700–5000 ppm range (*BS_3_1700, BS_3*, and *BS_3_5000* trials in Table 1) and under the exposure time of the step ii set at 3 h, as this was a duration previously known to render sterilization [16]. The sterilization process was effective for the three BIs up to a threshold value of H_2O_2 content (3300 ppm in *BS_3* trial). Other authors reported higher concentrations of chemical additives or even mixtures of

Table 1
Sterilization efficacy tests were carried out with different injected additive concentrations, exposure times and stirring modes marked with an (s). For notation, please refer to Section 3.1.

Test	Supercritical drying steps			H_2O_2 (ppm)	SAL-6 for *B. stearothermophilus*	SAL-6 for *B. atrophaeus*	SAL-6 for *B. pumilus*
	Step i	Step ii	Step iii				
Blank	2.0 h	1.0 h	1.5 h	0	**NO**	**NO**	**NO**
BS_3_1700	2.0 h	3.0 h (s)	1.5 h (s)	1700	YES	YES	**NO**
BS_3	2.0 h	3.0 h (s)	1.5 h (s)	3300	YES	YES	YES
BS_3_5000	2.0 h	3.0 h (s)	1.5 h (s)	5000	YES	YES	YES
BS_2	2.0 h	2.0 h (s)	1.5 h (s)	3300	YES	YES	YES
BS_1	2.0 h	1.0 h (s)	1.5 h (s)	3300	YES	YES	YES
BS_1_0	2.0 h	1.0 h (s)	1.5 h (s)	0	**NO**	**NO**	**NO**
B_3	2.0 h	3.0 h (s)	1.5 h	3300	YES	YES	YES
B_2	2.0 h	2.0 h (s)	1.5 h	3300	YES	YES	YES
B_1	2.0 h	1.0 h (s)	1.5 h	3300	YES	YES	**NO**
N_3	2.0 h	3.0 h	1.5 h	3300	YES	YES	**NO**
N_2	2.0 h	2.0 h	1.5 h	3300	YES	**NO**	**NO**
N_1	2.0 h	1.0 h	1.5 h	3300	YES	**NO**	**NO**

several compounds as additives (e.g·H_2O_2/HAc) to reach similar sterilization levels [41].

Lower additive contents (*BS_3_1700* trial) resulted in SAL-6 levels for *B. stearothermophilus* and *B. atrophaeus*, but this SAL-level was not achieved for *B. pumilus*. This result endorses the superior resistance of the latter BI against inactivation. Therefore, *B. pumilus* is recommended to be used as the BI for this sterilization technique and this decision may invalidate other SAL-6 sterilization conditions previously reported in the literature but evaluated with different BIs [12,41–43].

3.2.2. Exposure time effect

The impact of different exposure times (1, 2, and 3 h) during the step ii was assessed (*BS_1*, *BS_2* and *BS_3* tests in Table 1). Sterility was achieved in all cases and for all BIs. Although shorter times may be effective for sterilization, the minimum threshold was not sought because 1 hour was already the minimum time possible for effective supercritical drying of gels. Although the overall process lasted 4.5 h, the sterilization treatment after H_2O_2 injection only took 2.5 h. This duration is considered as very attractive for this case study of sterile aerogel production since shorter sterilization times were reported as effective only under harsher operational pressure and temperature conditions, and with weaker BIs (1 h in presence of water at 200 bar and 55 °C, achieving SAL-6 of a liquid suspension of *B. pumilus*) [12,39,42–44].

3.2.3. Stirring effect

Stirring is a commonly used parameter in supercritical sterilization protocols [20,32,43]. In this work, agitation was also relevant to reach the required sterility efficacy levels. Sterilization in the absence of stirring (*N_1,* Table 1) was only effective for *B. stearothermophilus* after a 1-h treatment, whereas prolonged times (3 h) were needed to reach SAL-6 levels for *B. atrophaeus* and even longer times are needed for *B. pumilus* (not sterilized after 3 h). Once again, *B. pumilus* is unveiled as the most resistant microorganism.

The stirring on the step ii increased the efficacy of the sterilization. Trials with stirring in step ii (*B_3*, *B_2* and *B_1* tests in Table 1) were able to inactivate BIs more effectively when compared to the counterpart trials without stirring (*N_3*, *N_2* and *N_1* tests). The sterility of the three BIs was achieved in the *B_2* and *B_3* trials, but for *B_1* trial just the *B. pumilus* spore strips were not sterilized. Tests with the stirring only in step ii resulted in SAL-6 levels for the three BIs after 3.5 h of H_2O_2 injection (*B_2* test). Stirring during the steps ii and iii accelerated the sterilization process with respect to the stirring only in the static step ii and SAL-6 levels were achieved after 2.5 h of H_2O_2 injection (*BS_1* test).

In the radar chart of Fig. 3, the conditions of pressure, temperature, process duration and sterilization effectiveness in relation to the BIs of *BS_1* trial (shown in green) were visually compared to other sterilization conditions found in the literature [12,14]. For the sake of comparison, the grey shaded area in Fig. 3 represented the conventional aerogel drying conditions used in our laboratory, which provide (unsterile) aerogels with excellent properties for both polymers (starch and alginate). The operating conditions of BS_1 trials (pressure, temperature, duration) were very close to those aerogel drying conditions deemed as optimal for in situ sterilization. Alternatively, other reported options of sterilization conditions have advantages for at least one operating parameter, namely in terms of lower processing time (Zani *et al.* [12], orange area) or temperature (Bento et al. [14]., pink area), but none of them guarantee the sterilization efficacy against standard BIs.

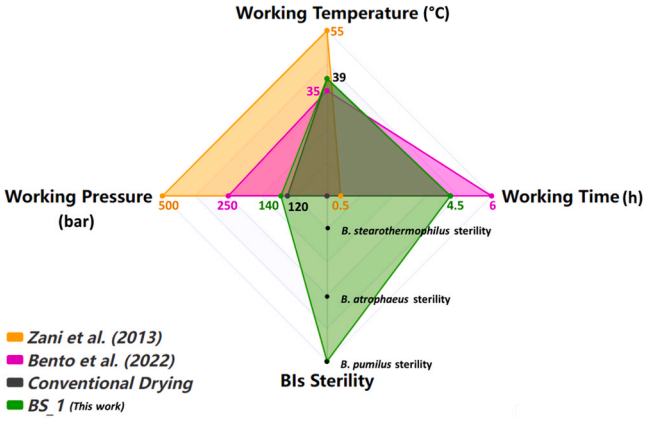

Fig. 3. Radar chart comparing different operational conditions and results for supercritical sterilization of aerogels. *Working pressure* was represented between 0 and 500 bar, *Working temperature* was ranged between 0 and 55°C, *Working time* was represented between 0 and 6 h, and *BIs sterility* was sorted from lower to higher resistance against $scCO_2$ sterilization, being *B. pumilus* the most resistant.

3.3. Physicochemical characterization of treated starch and alginate aerogels

The textural properties of starch and alginate aerogels dried in thermosealed pouches and aerogels treated in situ by modified drying protocols with H_2O_2 injection under different working conditions (Table 1) were studied. The sample denoted as *Blank* was produced using 3 bar/min as depressurization rate and in the absence of agitation and H_2O_2 for the sake of comparison of this typical supercritical drying procedure with other integrated sterilization trials under the same depressurization rates.

Overall porosity, A_{BET}, V_V and D_P of the resulting aerogels were measured, and the morphological appearance was observed by SEM microscopy. The effects of additive content, exposure time, stirring time and depressurization rate used in the experimental trials on the textural properties of the obtained aerogels were studied.

3.3.1. Additive use and depressurization rate effects on the textural properties of sterilized aerogels

The impact of the use of H_2O_2 chemical additive on the texture of the starch and alginate aerogels was analyzed under the less severe conditions in terms of H_2O_2 content (3300 ppm) able to give rise to SAL-6 levels for *B. pumilus* (i.e. *BS_1* test). Textural results for these aerogels (Fig. 4) were compared to the unsterile aerogels prepared either under the same conditions but without H_2O_2 (*BS_1_0* test) or under conventional supercritical drying conditions (*Blank* test). The porosity of starch aerogels had similar values for all the cases (Fig. 4a), with no significant differences between them. In the case of alginate aerogels, no significant differences were shown between the *Blank* and *BS_1_0* tests, but there were differences with regard to the *BS_1* test.

A_{BET} and V_v values of the sterile aerogels (Fig. 4b,c) were lower than their unsterile counterparts in this work, particularly for starch aerogels when compared to the *Blank* test. The addition of H_2O_2 during the in situ sterilization process as water:H_2O_2 mixtures might result in variations of the structural water present in the starch aerogel backbone and in increased capillary forces upon drying resulting in textural changes. Moreover, in the *in situ* sterilization treatments, the depressurization rate was three times higher than in the conventional drying process (1 bar/min). This faster decompression had an effect on the textural properties, in particular on the reduction of A_{BET} depending on the aerogel source. Conventionally dried starch aerogels (depressurized at 1 bar/min) showed an A_{BET} value of 261 ± 13 m^2/g, with no significant difference with respect to the *Blank* starch. Meanwhile, the A_{BET} of the alginate aerogels under conventional drying conditions (depressurized at 1 bar/min) was 366 ± 18 m^2/g, which is 44.8 % higher than in *Blank* alginate aerogels. The starch aerogel values of V_v (Fig. 4c) had no significant differences with respect to the blank. Regarding the distribution between meso and macropores, an increase in the volume of macropores in the starch aerogels was detected and likely related to the use of stirring in *BS_1* and *BS_1_0* trials. The increase in macroporosity was more

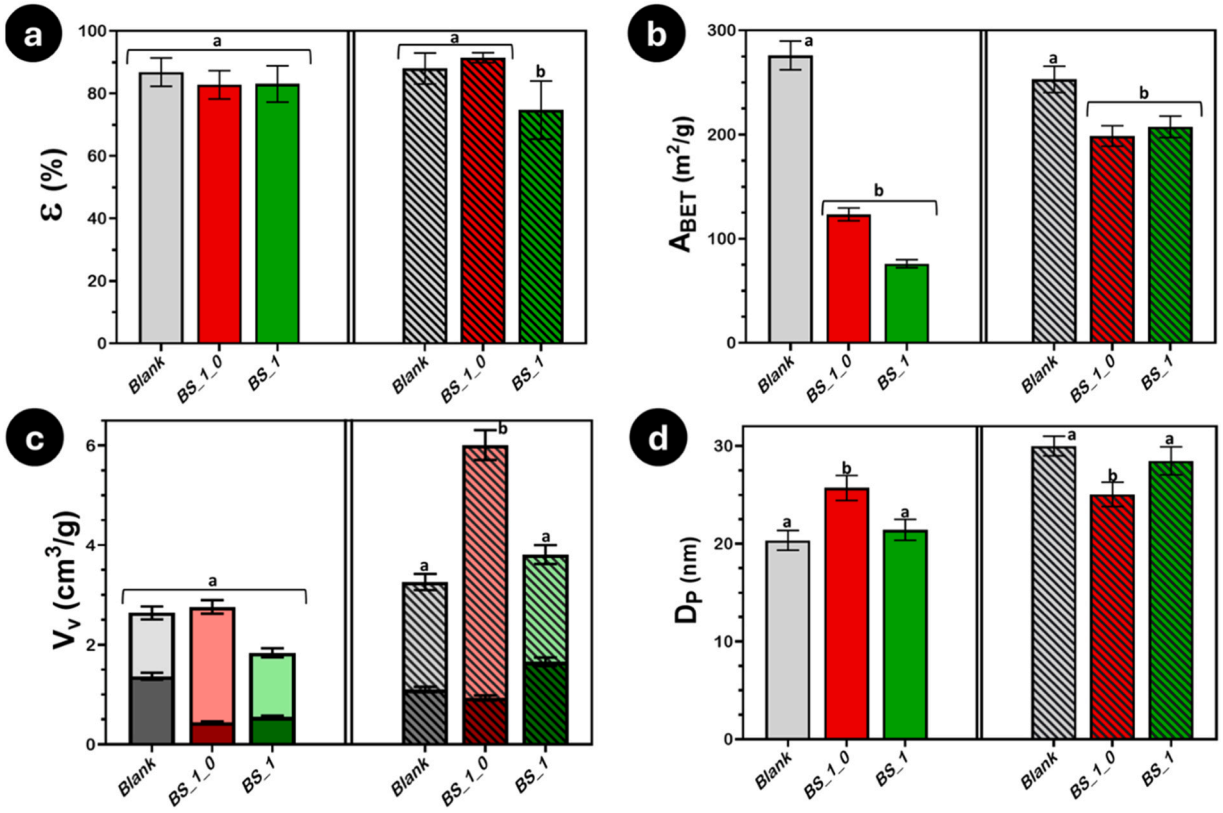

Fig. 4. Effect of the supercritical drying and sterilization in the presence of H_2O_2 additive (3300 ppm) on the textural properties of the starch aerogels monoliths (solid bars) and alginate aerogel beads (stripped bars): (a) overall porosity, (b) specific surface area, (c) total void pore volume, represented as the sum of macropore volume (light color) and mesopore volume (dark color), and (d) mean pore diameter. Red bars represent that SAL-6 level was not achieved in the trial, while the green bars are sterile experiments. Grey bars represent the *Blank* test. Equal letters denoted statistically homogeneous groups.

pronounced for the *BS_1_0* trial in aerogels based on alginate, while there was no significant difference between *Blank* and *BS_1* trials.

In comparison with the literature, A_{BET} and V_v values of the sterile aerogels were close to the typical values of non-sterile starch and alginate aerogels [16,45–47]. A_{BET} values for starch aerogels are typically between 71 and 209 m^2/g and porosities between 48 % and 81 % [47]. In this work, sterile aerogels with an A_{BET} of 76 m^2/g and porosities of 83 % were obtained when using the optimal *in situ* sterilization conditions (BS_1 trial). In contrast, the estimated values for non-sterile alginate aerogels are typically between 271 and 420 m^2/g [34]. The A_{BET} value obtained in this work for alginate aerogels (207 m^2/g) are in close proximity to those of the non-sterile alginate aerogels.

The SEM images of the alginate and starch aerogels under these three experimental conditions showed the highly porous and fibrous network structure of the gels with well-defined mesopores (Fig. 5), typical for aerogels. Aerogels from *BS_1_0* and *BS_1* showed a higher presence of

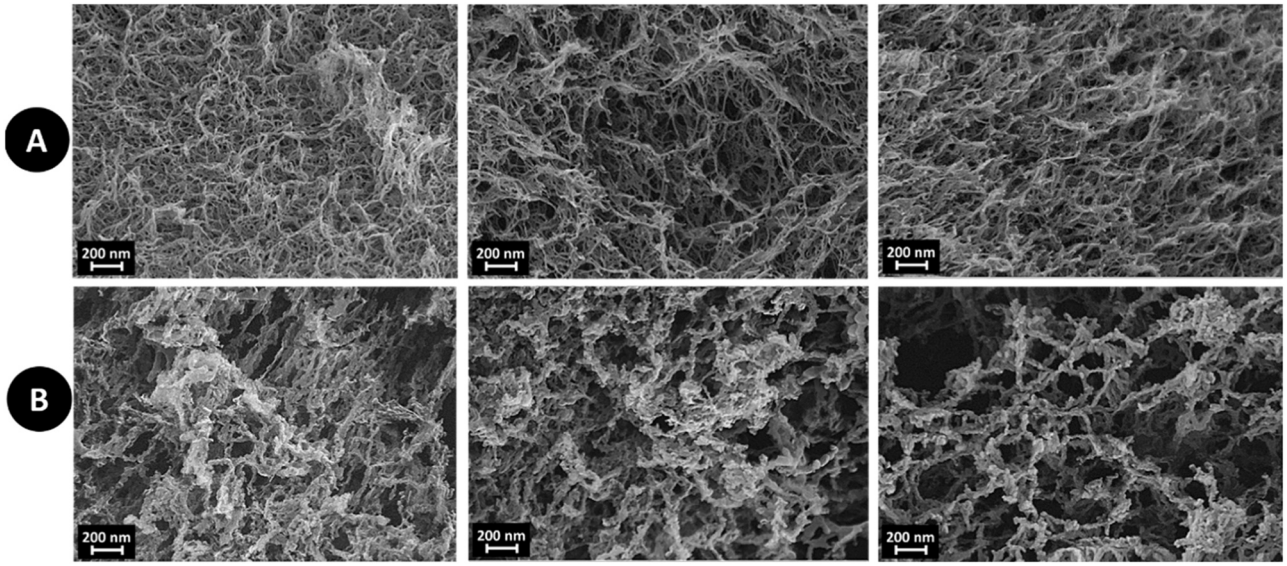

Fig. 5. SEM images of (A) alginate and (B) starch aerogels obtained by Blank (left), BS_1_0 (centre) and BS_1 (right) trial conditions.

macropores likely arising from the presence of stirring used in these trials. This is in accordance with the results obtained from the analysis of the textural properties shown in Fig. 4. No chemical changes were observed in the aerogels after the in situ sterilization process according to the FT-IR analyses (Fig. S1).

3.3.2. *Exposure time effect on the textural properties of sterilized aerogels*

Sterile aerogels fabricated with different step ii exposure times (1–3 h), and agitation during steps ii and iii were characterized (Fig. 6). Although sterile conditions were obtained for the three exposure times tested, a proportional and detrimental effect of longer exposure times on the textural properties of both biopolymer aerogels was unveiled.

The presence of water in the chemical additive may interfere in the gel drying process, as the H_2O_2 additive was added to the autoclave using commercial aqueous solutions (30 % w/w). Despite water being scarcely soluble in $scCO_2$ (4.9×10^{-3} mole fraction at 140 bar and 39°C), it can still be dissolved in the supercritical medium at low amounts and then bond to the hydrophilic polymeric chains of the starch and alginate gel matrices with high affinity to water [48]. It is expected that longer exposure times will result in higher amounts of water adsorbed in the polysaccharide gels. Water adsorption was also favored by the stirring during step ii, which increased the solubilization rate of water in $scCO_2$ and enhanced the adsorption of water in the gel structure of the aerogel. A higher water content in the gels will ultimately result in inferior textural properties as capillary forces cannot be totally avoided during this drying process in the presence of water. Accordingly, the textural values of the aerogels decreased with exposure time and those obtained for starch aerogels in *BS_3* test are very low and similar to other values reported in the literature for incomplete drying [25].

3.3.3. *Stirring effect on the textural properties of sterilized aerogels*

Being stirring a critical parameter to reach sterility (cf. Section 3.2), the effect of stirring on the textural properties of the aerogels was evaluated (Fig. 7). Aerogels treated with agitation in stages ii and iii (BS_1 trials) had the lowest values for all the textural parameters, while aerogels prepared without agitation (N_1 trials) had the highest ones. These results were related to the effect of the dynamic regime in stage iii to the end material properties. During this stage there is a continuous CO_2 flow that allows the extraction of residual EtOH and H_2O_2.

This behaviour is antagonized by the agitation that enhances a constant homogenization in the $scCO_2$ and retards the extraction of EtOH and H_2O_2 from the bottom of the autoclave. Accordingly, stirring only in the static step ii is advantageous in our experimental setup with respect to the stirring during the steps ii and iii, as the stirring during step iii will increase the H_2O_2 residence time in the autoclave and delay the removal of the excess of H_2O_2 from the supercritical medium.

Under the best conditions tested in this work (*BS_1* trial), the porosity decreased by *ca.* 7 % for starch and *ca.* 19 % for alginate with respect the unsterilized aerogel counterparts. A decrease in porosity by 29 % in alginate-gelatin aerogels was previously reported when pressurization-depressurization cycles were used during the supercritical drying process to effectively inactivate the presence of microorganisms (*Bacillus rhizosphaerae* and *Bacillus oceani*) in the polymer [14]. The sterilization by in situ sterilization enhanced with H_2O_2 seems to lead to superior textural properties than those obtained by sterilization enhanced with pressurization-depressurization cycles.

3.4. *In vitro compatibility sterilized aerogels*

After verifying the effectiveness of the integration of sterilization within the conventional drying process and ensuring that the textural properties of the materials were not significantly altered, the next challenge was to verify the biological safety of these materials using *in vitro* cell tests with fibroblasts. Results demonstrated that starch and

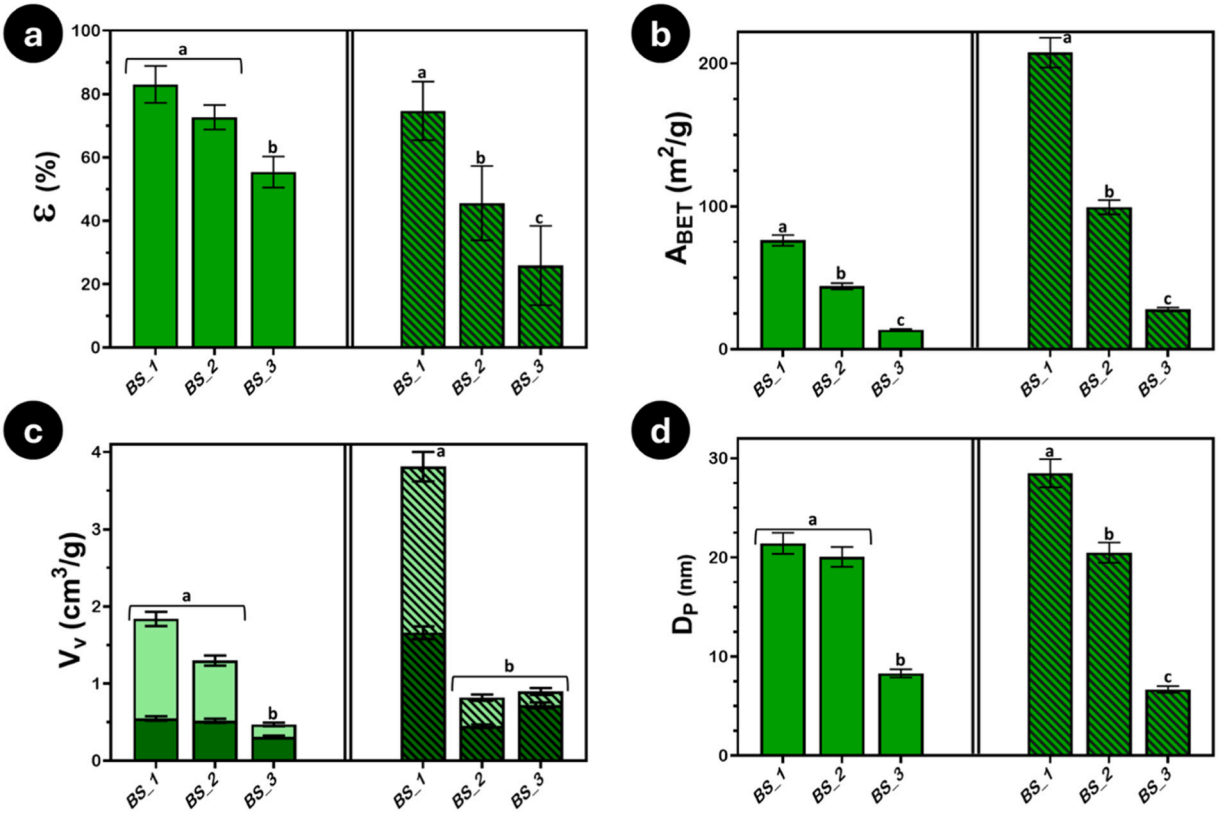

Fig. 6. Effect of exposure time on the textural properties of the sterile starch aerogel monoliths (solid bars) and alginate aerogel beads (stripped bars): (a) overall porosity, (b) specific surface area, (c) total void pore volume, represented as the sum of macropore volume (light color) and mesopore volume (dark color), and (d) mean pore diameter. Green bars represent that SAL-6 levels was achieved under the trial conditions. Equal letters denoted statistically homogeneous groups.

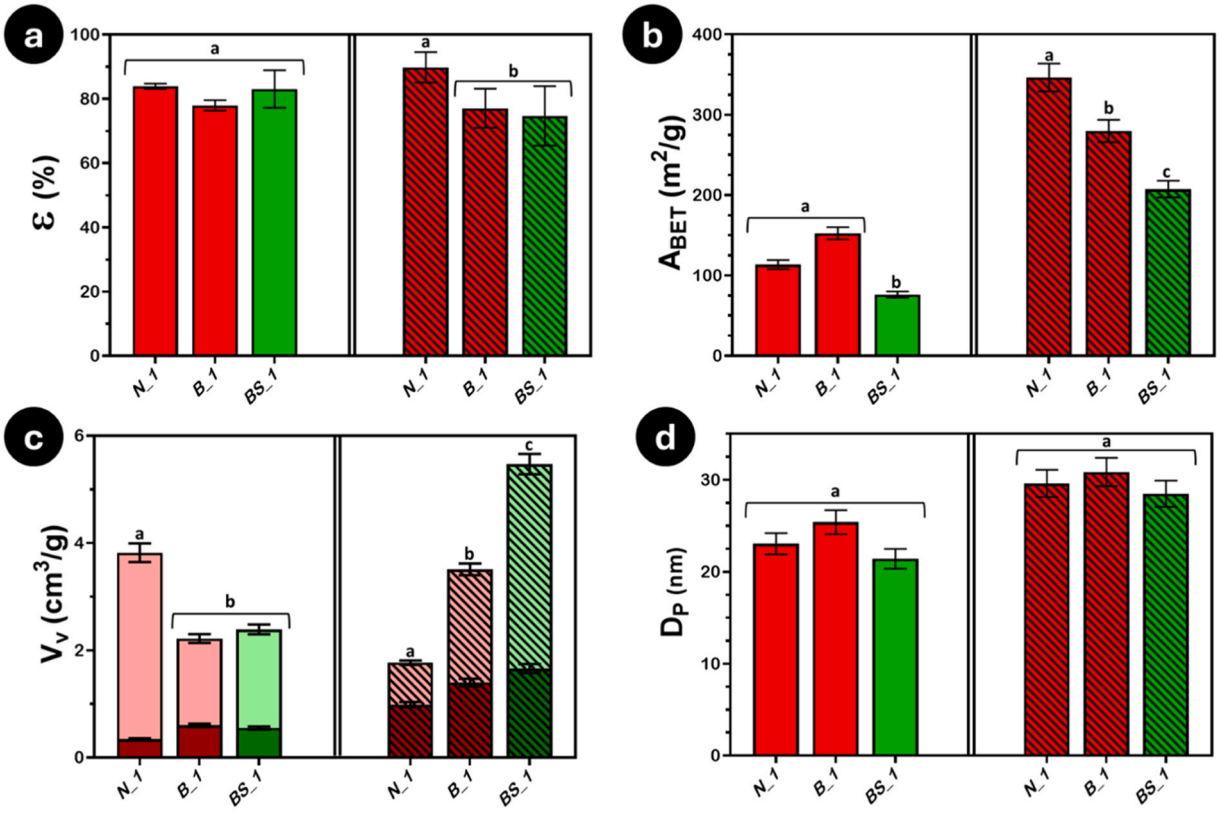

Fig. 7. Effect of the stirring time on the textural properties of starch aerogel monoliths (solid bars) and alginate aerogel beads (stripped bars): (a) overall porosity, (b) specific surface area, (c) total void pore volume, represented as the sum of macropore volume (light color) and mesopore volume (dark color), and (d) mean pore diameter. Red bars represent that SAL-6 level was not achieved, while green bars are sterile experiments. Equal letter denoted statistically homogeneous groups.

alginate aerogels manufactured in the presence of H_2O_2 (*BS_1* trial) were non-cytotoxic after 24 h and 48 h, since values of cells viability were higher than 80 % and with no significant differences with respect to the control (Fig. 8). This assay contributes to the evidence of the safety of these biomaterials using this sterilization approach.

4. Conclusions

Ready-to-use sterile aerogel materials at SAL-6 levels were directly produced using an integrated manufacturing process based on supercritical fluid technology. The use of CO_2 with the dual role as a sterilizing and extracting agent represents a green and sustainable method for the processing of sterile advanced materials with complex nanostructures that were unmet so far in certain cases. Sterile starch and alginate aerogels were successfully obtained in 4.5 h under the optimal conditions, operating at pressures between 120 and 140 bar and at a constant temperature of 39°C. *Bacillus pumilus* was found to be the most resistant microorganism to this sterilization technique. The texture performance of starch and alginate aerogels was within the typical range of aerogels and comparable to those from aerogels produced through the

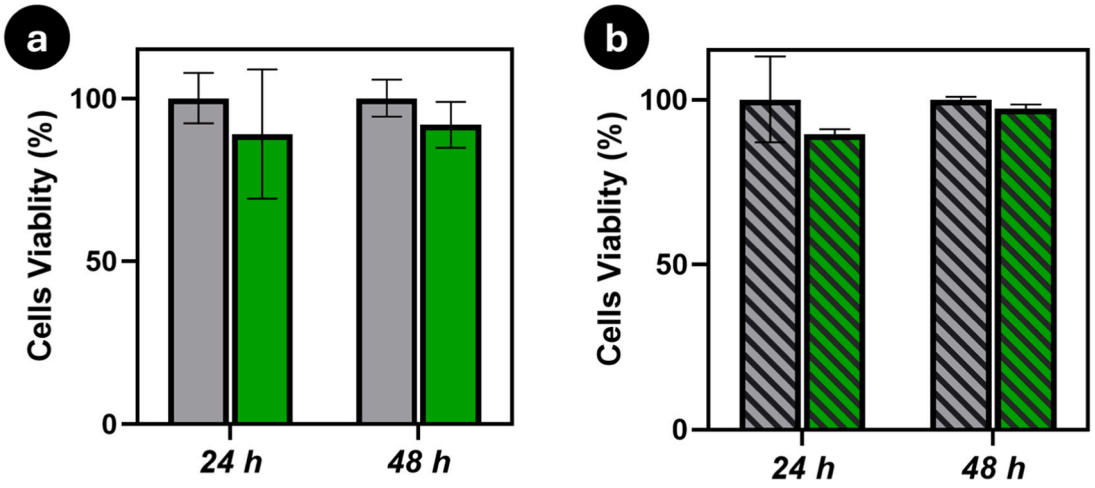

Fig. 8. Cell viability studies expressed in percentage determined after 24 and 48 h of contact with sterile aerogels formulations (a) solid bars are for starch aerogels and (b) striped bars are for alginate. Gray bars are aerogels related to *BS_1_0* trial and green bars corresponded to *BS_1* trial. No statistical differences were obtained among samples.

conventional drying method under non-sterile conditions. This integration of the sterilization during the aerogel production may result in economic costs reduction and potential risks of contamination of biomaterials by handling can be avoided. Finally, the presence of residual H_2O_2 in the aerogels was imperceptible and, as a result, these aerogels were cytocompatible with fibroblastic cell lines. These results confirm the feasibility of the *in situ* sterilization of aerogels and open up new possibilities on the use of aerogels as scaffolds for tissue engineering or as carriers in pharmaceutical formulations requiring controlled sterilization levels.

CRediT authorship contribution statement

Clara López-Iglesias: Methodology, Writing – review & editing. **Carlos A García-González:** Writing – review & editing, Writing – original draft, Supervision, Methodology, Investigation, Funding acquisition, Conceptualization. **Beatriz Magariños:** Writing – review & editing, Supervision, Methodology, Investigation, Funding acquisition, Conceptualization. **Inés Ardao:** Writing – review & editing, Methodology, Investigation. **María Carracedo-Pérez:** Writing – review & editing, Writing – original draft, Methodology, Investigation.

Declaration of Competing Interest

All authors disclose no actual or potential conflict of interest related with any financial and personal relationships with other people or organizations that could inappropriately influence, or be perceived to influence, this work.

Data availability

Data will be made available on request.

Acknowledgements

This work was funded by MICIU/AEI/10.13039/501100011033 [grants PID2020–120010RB-I00 and PDC2022–133526-I00], Xunta de Galicia [ED431C2022/2023], Xunta de Galicia-GAIN [Ignicia Programme 2021, ECOBONE], ERDF/EU and European Union NextGenerationEU/PRTR. C. L.-I. acknowledges Xunta de Galicia for a postdoctoral fellowship [ED481B-2021–008]. Work carried out in the framework of the ECO-AERoGELS COST Innovators' Grant (ref. IG18125) and funded by the European Commission.

Appendix A. Supporting information

Supplementary data associated with this article can be found in the online version at doi:10.1016/j.jcou.2024.102891.

References

[1] International Union Of pure and applied chemistry IUPAC, Announces the 2022 top ten emerging the technologies in chemistry, IUPAC Announc. 2022 Top. Ten Emerg. Technol. Chem. (2023).
[2] J. Stergar, U. Maver, Review of aerogel-based materials in biomedical applications, J. Sol-Gel Sci. Technol. 77 (2016) 738–752, https://doi.org/10.1007/s10971-016-3968-5.
[3] C.A. García-González, A. Sosnik, J. Kalmár, I.D. Marco, C. Erkey, A. Concheiro, C. Alvarez-Lorenzo, Aerogels in drug delivery: from design to application, J. Controll. Release 332 (2021) 40–63, https://doi.org/10.1016/j.jconrel.2021.02.012.
[4] B.G. Bernardes, P. Del Gaudio, P. Alves, R. Costa, C.A. García-González, A. L. Oliveira, Bioaerogels: promising nanostructured materials in fluid management, healing and regeneration of wounds, Molecules 26 (2021) 3834, https://doi.org/10.3390/molecules26133834.
[5] E.B. Yahya, A.A. Amirul, H.P.S., A.K, N.G. Olaiya, M.O. Iqbal, F. Jummaat, A.K., A. S, A.S. Adnan, Insights into the role of biopolymer aerogel scaffolds in tissue engineering and regenerative medicine, Polymers *13* (2021) 1612, https://doi.org/10.3390/polym13101612.
[6] I. Lázár, L. Čelko, M. Menelaou, Aerogel-based materials in bone and cartilage tissue engineering—a review with future implications, Gels *9* (2023) 746, https://doi.org/10.3390/gels9090746.
[7] T. Ferreira-Gonçalves, A. Iglesias-Mejuto, T. Linhares, J.M.P. Coelho, P. Vieira, P. Faísca, J. Catarino, P. Pinto, D. Ferreira, H.A. Ferreira, et al., Biological thermal performance of organic and inorganic aerogels as patches for photothermal therapy, Gels *8* (2022) 485, https://doi.org/10.3390/gels8080485.
[8] S. Basak, R.S. Singhal, The potential of supercritical drying as a "green" method for the production of food-grade bioaerogels: a comprehensive critical review, Food Hydrocoll. *141* (2023) 108738, https://doi.org/10.1016/j.foodhyd.2023.108738.
[9] M. Guastaferro, E. Reverchon, L. Baldino, Agarose, alginate and chitosan nanostructured aerogels for pharmaceutical applications: a short review, Front. Bioeng. Biotechnol. *9* (2021) 688477, https://doi.org/10.3389/fbioe.2021.688477.
[10] J. Feng, B.-L. Su, H. Xia, S. Zhao, C. Gao, L. Wang, O. Ogbeide, J. Feng, T. Hasan, Printed aerogels: chemistry, processing, and applications, Chem. Soc. Rev. *50* (2021) 3842–3888, https://doi.org/10.1039/C9CS00757A.
[11] T. Duong, C. López-Iglesias, P.K. Szewczyk, U. Stachewicz, J. Barros, C. Alvarez-Lorenzo, M. Alnaief, C.A. García-González, A pathway from porous particle technology toward tailoring aerogels for pulmonary drug administration, Front. Bioeng. Biotechnol. *9* (2021) 671381, https://doi.org/10.3389/fbioe.2021.671381.
[12] F. Zani, C. Veneziani, E. Bazzoni, L. Maggi, G. Caponetti, R. Bettini, Sterilization of Corticosteroids for Ocular and Pulmonary Delivery with Supercritical Carbon Dioxide, Int. J. Pharm. *450* (2013) 218–224, https://doi.org/10.1016/j.ijpharm.2013.04.055.
[13] N. Ribeiro, G.C. Soares, V. Santos-Rosales, A. Concheiro, C. Alvarez-Lorenzo, C. A. García-González, A.L. Oliveira, A new era for sterilization based on supercritical CO_2 technology, J. Biomed. Mater. Res. B Appl. Biomater. 108 (2020) 399–428, https://doi.org/10.1002/jbm.b.34398.
[14] C.S.A. Bento, S. Alarico, N. Empadinhas, H.C. de Sousa, M.E.M. Braga, Sequential $scCO_2$ drying and sterilisation of alginate-gelatine aerogels for biomedical applications, J. Supercrit. Fluids 184 (2022) 105570, https://doi.org/10.1016/j.supflu.2022.105570.
[15] T. Carranza, M. Zalba-Balda, M.J. Barriola Baraibar, P. Guerrero, K. de la Caba, Effect of sterilization processes on alginate/gelatin inks for three-dimensional printing, Int. J. Bioprinting 9 (2022) 645, https://doi.org/10.18063/ijb.v9i1.645.
[16] V. Santos-Rosales, I. Ardao, C. Alvarez-Lorenzo, N. Ribeiro, A. Oliveira, C. García-González, Sterile and dual-porous aerogels scaffolds obtained through a multistep supercritical CO2-based approach, Molecules *24* (2019) 871, https://doi.org/10.3390/molecules24050871.
[17] M. Carracedo-Pérez, B. Magariños, C.A. García-González, Strategies for the Sterilization of Polymeric Biomaterials. In *Polymeric Materials for Biomedical Implants*, Elsevier, 2024, pp. 547–583. ISBN 978-0-323-99690-7.
[18] R.E. Harrington, T. Guda, B. Lambert, J. Martin, Sterilization and Disinfection of Biomaterials for Medical Devices. In *Biomaterials Science*, Elsevier, 2020, pp. 1431–1446. ISBN 978-0-12-816137-1.
[19] A. Kucharska-Jastrząbek, E. Chmal-Fudali, D. Rudnicka, B. Kosińska, Effect of sterilization on bone implants based on biodegradable polylactide and hydroxyapatite, Materials *16* (2023) 5389, https://doi.org/10.3390/ma16155389.
[20] A. Iglesias-Mejuto, C.A. García-González, 3D-printed, dual crosslinked and sterile aerogel scaffolds for bone tissue engineering, Polymers *14* (2022) 1211, https://doi.org/10.3390/polym14061211.
[21] T. Yang, B. Dou, H. Zhang, K. Wu, N. Luo, H. Chen, Y. Xu, W. Li, C. Wu, Novel design of In-Situ hydrogen sorption/storage integrated enhanced hydrogen production in supercritical CO_2 gasification, air gasification, and steam gasification from biomass, Chem. Eng. J. 485 (2024) 150029, https://doi.org/10.1016/j.cej.2024.150029.
[22] X. Kang, L. Mao, J. Shi, Y. Liu, B. Zhai, J. Xu, Y. Jiang, E. Lichtfouse, H. Jin, L. Guo, Supercritical carbon dioxide systems for sustainable and efficient dissolution of solutes: a review, Environ. Chem. Lett. *22* (2024) 815–839, https://doi.org/10.1007/s10311-023-01681-4.
[23] L. Garcia-Gonzalez, A.H. Geeraerd, S. Spilimbergo, K. Elst, L. Van Ginneken, J. Debevere, J.F. Van Impe, F. Devlieghere, High pressure carbon dioxide inactivation of microorganisms in foods: the past, the present and the future, Int. J. Food Microbiol. *117* (2007) 1–28, https://doi.org/10.1016/j.ijfoodmicro.2007.02.018.
[24] A. Tabernero, Á. González-Garcinuño, S. Cardea, E. Martín Del Valle, Supercritical carbon dioxide and biomedicine: opening the doors towards biocompatibility, Chem. Eng. J. *444* (2022) 136615, https://doi.org/10.1016/j.cej.2022.136615.
[25] C.A. García-González, M.C. Camino-Rey, M. Alnaief, C. Zetzl, I. Smirnova, Supercritical drying of aerogels using CO_2: effect of extraction time on the end material textural properties, J. Supercrit. Fluids 66 (2012) 297–306, https://doi.org/10.1016/j.supflu.2012.02.026.
[26] A. Bueno, I. Selmer, R. S.P, P. Gurikov, W. Lölsberg, D. Weinrich, M. Fricke, I. Smirnova, First evidence of solvent spillage under subcritical conditions in aerogel production, Ind. Eng. Chem. Res. *57* (2018) 8698–8707, https://doi.org/10.1021/acs.iecr.8b00855.
[27] İ. Şahin, Y. Özbakır, Z. İnönü, Z. Ulker, C. Erkey, Kinetics of supercritical drying of gels, Gels *4* (2017) 3, https://doi.org/10.3390/gels4010003.
[28] C.A. García-González, I. Smirnova, Use of supercritical fluid technology for the production of tailor-made aerogel particles for delivery systems, J. Supercrit. Fluids *79* (2013) 152–158, https://doi.org/10.1016/j.supflu.2013.03.001.
[29] G.C. Soares, D.A. Learmonth, M.C. Vallejo, S.P. Davila, P. González, R.A. Sousa, A. L. Oliveira, Supercritical CO^2 technology: the next standard sterilization technique?

Mater. Sci. Eng. C. 99 (2019) 520–540, https://doi.org/10.1016/j.msec.2019.01.121.
[30] V. Warambourg, A. Mouahid, C. Crampon, A. Galinier, M. Claeys-Bruno, E. Badens, Supercritical CO_2 sterilization under low temperature and pressure conditions, J. Supercrit. Fluids 203 (2023) 106084, https://doi.org/10.1016/j.supflu.2023.106084.
[31] V. Santos-Rosales, B. Magariños, C. Alvarez-Lorenzo, C.A. García-González, Combined sterilization and fabrication of drug-loaded scaffolds using supercritical CO_2 technology, Int. J. Pharm. 612 (2022) 121362, https://doi.org/10.1016/j.ijpharm.2021.121362.
[32] V. Santos-Rosales, B. Magariños, R. Starbird, J. Suárez-González, J.B. Fariña, C. Alvarez-Lorenzo, C.A. García-González, Supercritical CO_2 technology for one-pot foaming and sterilization of polymeric scaffolds for bone regeneration, Int. J. Pharm. 605 (2021) 120801, https://doi.org/10.1016/j.ijpharm.2021.120801.
[33] P. Remuiñán-Pose, C. López-Iglesias, A. Iglesias-Mejuto, J.F. Mano, C.A. García-González, M.I. Rial-Hermida, Preparation of vancomycin-loaded aerogels implementing inkjet printing and superhydrophobic surfaces, Gels *8* (2022) 417, https://doi.org/10.3390/gels8070417.
[34] R. Rodríguez-Dorado, C. López-Iglesias, C. García-González, G. Auriemma, R. Aquino, P. Del Gaudio, Design of aerogels, cryogels and xerogels of alginate: effect of molecular weight, gelation conditions and drying method on particles' micromeritics, Molecules *24* (2019) 1049, https://doi.org/10.3390/molecules24061049.
[35] AENOR *ISO 17665-1:2006 Sterilization of Health Care Products-Moist Heat-Part 1: Requirements for the Development, Validation and Routine Control of a Sterilization Process for Medical Devices*.
[36] AENOR *ISO 11135:2014 Sterilization of Health Care Products-Ethylene Oxide-Part 1: Requirements for the Development, Validation and Routine Control of a Sterilization Process for Medical Devices.*
[37] AENOR *ISO 11137-1:2006 Sterilization of Health Care Products-Radiation-Part 1: Requirements for Development, Validation and Routine Control of a Sterilization Process for Medical Devices.*
[38] A. Iglesias-Mejuto, B. Magariños, T. Ferreira-Gonçalves, R. Starbird-Pérez, C. Álvarez-Lorenzo, C.P. Reis, I. Ardao, C.A. García-González, Vancomycin-loaded methylcellulose aerogel scaffolds for advanced bone tissue engineering, Carbohydr. Polym. *324* (2024) 121536, https://doi.org/10.1016/j.carbpol.2023.121536.
[39] J.D. Hemmer, M.J. Drews, M. LaBerge, M.A. Matthews, Sterilization of bacterial spores by using supercritical carbon dioxide and hydrogen peroxide, J. Biomed. Mater. Res. B Appl. Biomater. *80B* (2007) 511–518, https://doi.org/10.1002/jbm.b.30625.
[40] R.R. Mallepally, M.A. Marin, N. Montesdeoca, C. Parrish, K.R. Ward, M.A. McHugh, Hydrogen peroxide loaded cellulose acetate mats as controlled topical O_2 delivery devices, J. Supercrit. Fluids 105 (2015) 77–83, https://doi.org/10.1016/j.supflu.2014.12.029.
[41] L. Andrée, J. Dodemont, H.R. Harhangi, K. Dijkstra, L. Niftrik, F. van; Yang, S.C. G. Leeuwenburgh, Inactivation of *Staphylococcus aureus* in gelatin nanoparticles using supercritical carbon dioxide, J. Supercrit. Fluids (2023) 105979, https://doi.org/10.1016/j.supflu.2023.105979.
[42] K.L. Delma, N. Penoy, B. Grignard, R. Semdé, B. Evrard, G. Piel, Effects of supercritical carbon dioxide under conditions potentially conducive to sterilization on physicochemical characteristics of a liposome formulation containing apigenin, J. Supercrit. Fluids *179* (2022) 105418, https://doi.org/10.1016/j.supflu.2021.105418.
[43] I. Donati, M. Benincasa, M.-P. Foulc, G. Turco, M. Toppazzini, D. Solinas, S. Spilimbergo, I. Kikic, S. Paoletti, Terminal sterilization of BisGMA-TEGDMA thermoset materials and their bioactive surfaces by supercritical CO_2, Biomacromolecules *13* (2012) 1152–1160, https://doi.org/10.1021/bm300053d.
[44] J. Zhang, T.A. Davis, M.A. Matthews, M.J. Drews, M. LaBerge, Y.H. An, Sterilization using high-pressure carbon dioxide, J. Supercrit. Fluids *38* (2006) 354–372, https://doi.org/10.1016/j.supflu.2005.05.005.
[45] P. Paraskevopoulou, I. Smirnova, T. Athamneh, M. Papastergiou, D. Chriti, G. Mali, T. Čendak, M. Chatzichristidi, G. Raptopoulos, P. Gurikov, Mechanically strong polyurea/polyurethane-cross-linked alginate aerogels, ACS Appl. Polym. Mater. *2* (2020) 1974–1988, https://doi.org/10.1021/acsapm.0c00162.
[46] M. Martins, A.A. Barros, S. Quraishi, P. Gurikov, S.P. Raman, I. Smirnova, A.R. C. Duarte, R.L. Reis, Preparation of macroporous alginate-based aerogels for biomedical applications, J. Supercrit. Fluids *106* (2015) 152–159, https://doi.org/10.1016/j.supflu.2015.05.010.
[47] I. Lukic, J. Pajnik, V. Tadic, S. Milovanovic, Supercritical CO_2-assisted processes for development of added-value materials: Optimization of starch aerogels preparation and hemp seed extracts impregnation, J. CO2 Util. 61 (2022) 102036, https://doi.org/10.1016/j.jcou.2022.102036.
[48] G. Leeke, F. Gaspar, R. Santos, Influence of water on the extraction of essential oils from a model herb using supercritical carbon dioxide, Ind. Eng. Chem. Res. *41* (2002) 2033–2039, https://doi.org/10.1021/ie010845z.